Strong increase in convective precipitation in response to higher temperatures
SUPPLEMENTARY INFORMATION

January 10, 2013

Peter Berg

Institute for Meteorology and Climate Research, Karlsruhe Institute of Technology, Karlsruhe
Now at Rossby Centre, Swedish Meteorological and Hydrological Institute, Norrköping, Sweden
peter.berg@smhi.se

Christopher Moseley

Max Planck Institute for Meteorology, Hamburg, Germany and Helmholtz Zentrum Geesthacht, Climate Service Center, Hamburg, Germany
christopher.moseley@zmaw.de

Jan O. Haerter

Center for Models of Life, Niels Bohr Institute, Copenhagen, Denmark
haerter@nbi.dk

In this supplementary information we provide additional background on our data and the analysis performed. This material is not essential for the understanding of the main text but does provide additional details for readers interested in technical aspects of the data, the assumptions made in its processing, and the sensitivity towards modifications of the procedures. In particular, we describe several additional aspects of the synoptic, precipitation gauge and radar data and describe the sensitivity tests performed to check for robustness of our analysis results. This material further provides additional figures that explore aspects of the separation of stratiform and convective precipitation not contained in

the main manuscript. We also offer additional discussions on the event correlation and relative humidity analysis.

Synoptic Data

Diurnal cycle in the synoptic data

The synoptic observations are dependent on the brightness conditions, so that observations can be made. Fig. S1 shows the total number of observations of the different types depending on the time of day for the period 2007–2008. The most striking feature is the number of missing data ("NaN") for the dark night hours. Thus, there is a clear day/night bias which is transferred to the classification of precipitation types. As convection is more common in daytime it is not affected as much as stratiform conditions. The latter follows the expected weak diurnal cycle, with a small peak in the early morning hours [1]. The durations of the events presented in the main text are mostly below 200 minutes, so the impact of the day/night bias on event durations can be considered low. Fig. S1 further shows a clear mid-afternoon increase of convective precipitation [1, 2]. The seasonal cycle of classified events shows a pronounced increase of the number of convective events in summer and almost no convective activity in winter. The largest number of convective (stratiform) events is recorded in July (January). The overall number of events (any classification) is relatively constant throughout the year.

Characterisation of mixed type precipitation intensity

Our classification of precipitation records by synoptic observations also includes mixed conditions which may contain both stratiform and convective precipitation. To investigate the relation of the mixed conditions, we reproduce Fig. 2 (main text), but also include the statistical data for mixed conditions (Fig. S2), which were left out of the main Fig. 2 for reasons of clarity. The overall behaviour here is that mixed conditions behave intermediate between strictly stratiform (shown in red) and strictly convective (shown in blue) conditions. This is in line with the co-existence of both stratiform and convective cloud types in the mixed conditions. Note also the close resemblance to the behaviour when including all data in the statistics (black dots and lines in Fig. S2a and c. From the dry probability (observational records
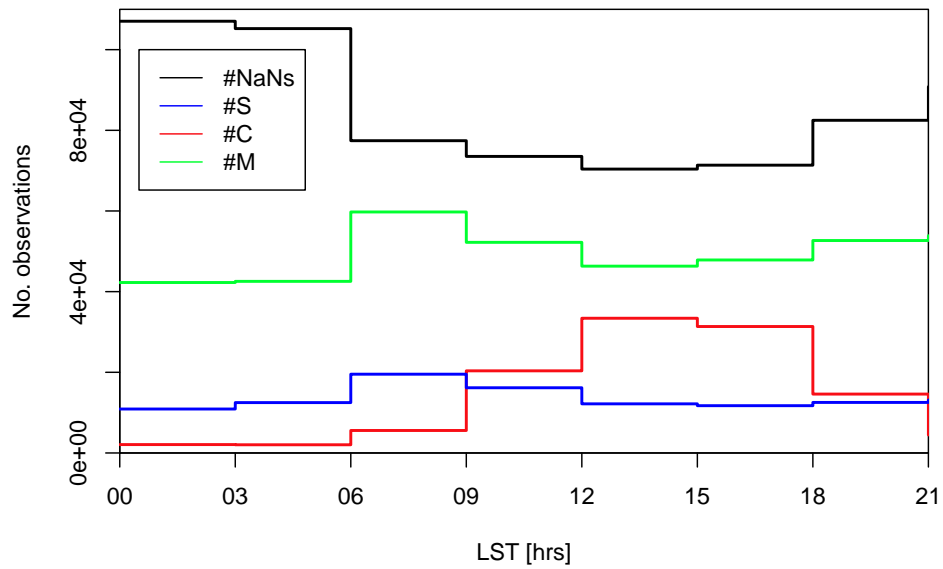
2

Figure S1: **Day/night bias of synoptic observations.** The total number of observations over Germany for 2007–2008, separated by their classification into stratiform (S), Convective (C), Mixed (M) and no available records (NaN), as a function of the time of day in local solar time (LST).
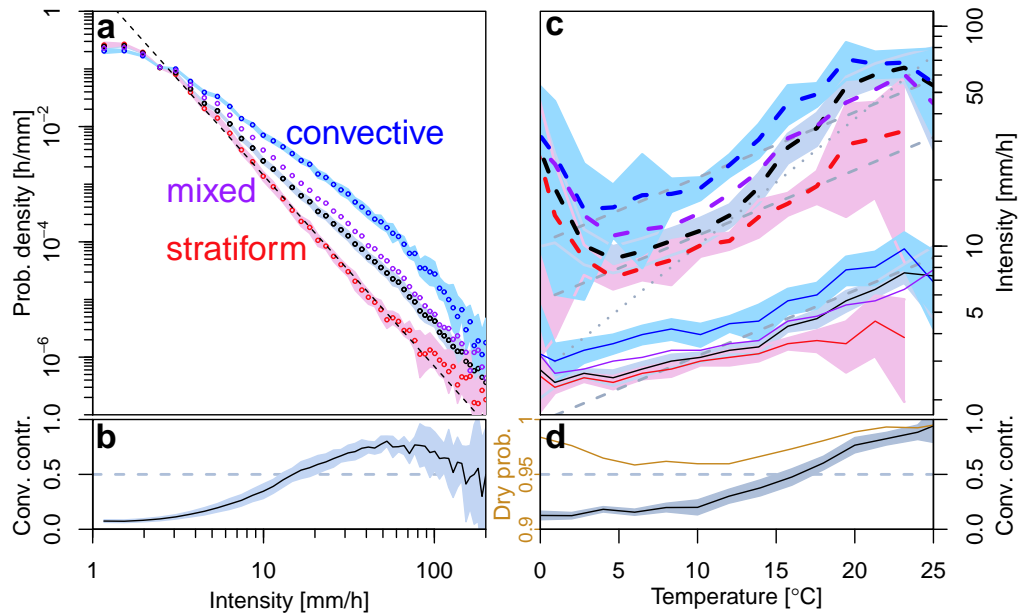
Figure S2: **Probability distribution of precipitation intensity.** Similar to Fig. 2 of the main text but including also mixed type precipitation (purple points and lines in panels a and c). In (d) we have further included the probability of a record being dry, i.e. with precipitation below the measurement threshold, shown as an orange line.

with less than 0.1 mm), shown in Fig. S2d, we conclude that the predominant number of 5-minute records shows no detectable precipitation. The highest probability of observing precipitation in the study region is for temperatures near 10°C at approximately four percent.

Rain gauge data

Sensitivity Tests

A number of sensitivity tests were carried out for the *ground-based precipitation gauge data*: The gauge analysis (main text Figs. 2 and 4) have been found

robust for variations of the lower limit in the range 0.01 to 0.5 mm/5 min, the time period before and after the synoptic observations in the range 15 to 90 min, using maximum or minimum temperature, and for variations of intermittancy (periods with precipitation below the threshold within an event) of 0 to 20 min. Additionally, the different criteria *Q1* and *Q2*, for the quadrant aggregated synoptic data, have some impact on main text Figs. 2 and 4 (see following section on Q1 and Q2 differences in this Supplementary Information). Further, it may be appropriate to use daily maximum temperature rather than the daily mean temperature [3, 4]. The result of using daily maximum temperature in the analysis, yields a figure similar to Fig. 2 (main text) but horizontally shifted to slightly higher temperatures. The super-Clausius-Clapeyron scaling for convective, but not for stratiform precipitation is preserved.

Q1 and *Q2* differences

For Fig. 2 of the main text, the *Q1* selection criteria was used. Using the *Q2*-criterion, the results are similar, although the stricter criterion leads to more noise. The main differences are at low temperatures for the convective type, and at high temperatures for the stratiform type. Again we find super-Clausius-Clapeyron scaling for the convective type but no indication of such scaling for the stratiform precipitation. The results of Fig. 2c (main text) should be compared also to Fig. S4 for the radar data and the strict *Q2*-criterion.

For the main text Fig. 4, the *Q2* criterium was used for clear separation of the types. The main difference between *Q1* and *Q2* is the relatively larger decrease in sample size for the convective compared to the stratiform type, which leads to a relative vertical shift of the distribution functions shown in Fig. 4a (main text). However, the shape of the curves is robust to the change of criterion. The temperature dependence of the convective event percentiles (Fig. 4e) is again beyond the Clausius-Clapeyron increase, but somewhat reduced compared to the stricter *Q2*-criterion. The latter can again be explained by sample contamination, as the convective starts to mimic the behaviour of the stratiform type.

5

Hourly resolution

For comparison to earlier work [3], we reproduce Fig. 2 of the main text for the hourly temporal resolution. Fig. S3 is consistent with both results presented in [3] and with proposed statistical explanations [5]. A super-Clausius-Clapeyron increase in convective and total precipitation arises also here for temperatures above approximately 12°C and the higher percentiles.

Radar Data

The radar data generally allow for much larger data coverage due to their high spatial resolution. Therefore, even at the stricter separation criterion *Q2*, all analyses showed relatively low statistical noise.

Sensitivity tests

The following sensitivity tests were carried out for the *radar data*:

- The separation of convective and stratiform events was performed for both the *Q1* and *Q2* classification criterium described in the Methods section of the main text. In the *Q1*-criterion approximately 2/3 (1/3) of the number of identified event areas correspond to the stratiform (convective) type. Using the *Q2*-criterium, the number of identified convective events drops to approximately 1/2 the amount and the number of stratiform events drops to approximately 1/5 the amount. The larger decrease in the amount of stratiform data is due to the large number of records with mixed conditions, which are often mixed with stratiform signals but less frequently with convective signals. When the criterion is switched from *Q2* to *Q1*, the result is that the probability distributions in Fig. 4c undergo relative vertical shifts. The overall shape of the curves remains nearly unchanged. Also, the curves in Fig. 4f remain very similar.

- For the calculation of the event sizes (second data package), the lower cutoff was reduced from 1.2 mm/h to 0.6 mm/h. The main effect of the inclusion of a greater number of low-intensity values is a reduction of the precipitation intensity curves in Fig. 4f and a general vertical shift. The overall shape of the curves remains similar.
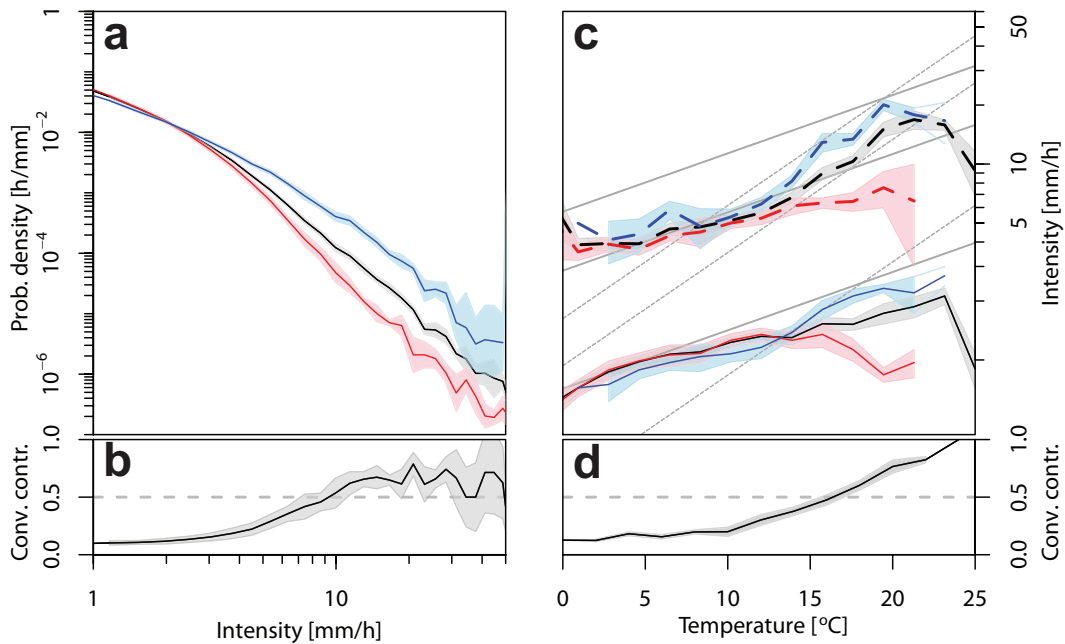
6

Figure S3: **Probability distribution of precipitation intensity at hourly resolution. a**, one-hour precipitation intensity distribution for convective (blue), stratiform (red) and total precipitation (black) from precipitation gauges. Note the double-logarithmic axes. **b**, The relative contribution of convective precipitation to the sum of the two types as function of intensity. Note the logarithmic horizontal scale. **c**, Intensity percentiles of convective (blue), stratiform (red) and total precipitation (black) for the 75th (solid) and 99th (dotted) percentiles. Solid (dotted) gray lines mark $7\%/^\circ C$ ($14\%/^\circ C$) increases. Note the logarithmic vertical axis. **d**, Same as (b) but as function of temperature. Shaded areas denote the 90% confidence intervals computed by bootstrapping.

7

- The station data were taken from the South-Western state of Baden-Württemberg in Germany. The radar measurements were available for all of Germany, hence in a comparison of the two data sets the radar data should be restricted to a similar area. We have used only radar data for the South of Germany in the main text. However, we have explored how the results would change if different constraints were made on the study region. In particular, we have compared the South only to the whole area of Germany. The differences were minor.

Intensity percentiles for the radar data

Fig. 2c (main text) was obtained for the precipitation gauge data. We ask whether similar features as presented there would also be visible in the radar data. In Fig. S4 we present corresponding percentiles for the radar data precipitation intensity as a function of temperature. In the figure we include now a larger number of percentiles, to address the temperature dependence over a larger range of the distribution function. Again, stratiform percentiles increase at rates approximately equal to the Clausius-Clapeyron rate of 7%/°C (Fig. S4a). Convective percentiles increase at higher rates for temperatures approximately larger than 15°C (Fig. S4b) and saturate near 22°C – again similar to the observations with station data in the main text. Note that in the figure even the lower percentiles of convective precipitation produce super-Clausius-Clapeyron increases with temperature.

Comparison with the bright band condition

Traditionally, a distinction of stratiform and convective conditions has been made by detection of a *bright band* in the radar reflectivity signal [6, 7, 8]. The bright band results from the changes in radar reflectivity when descending snow particles melt and become rain drops.

To make contact with this method, we present in Fig. S5 time series of vertical records [9] of radar reflectivity, vertical velocity and rain rate at the Lindenberg site (marked in main text Fig. 1a) outside of Berlin, located in the North-Eastern quadrant of our study area [9]. Fig. S5a-c shows an example of the radar reflectivity records for the stratiform classification. This event corresponds to the 6 pm radar image shown in Fig. 1b, main text, where widespread stratiform conditions are present in the North-Eastern quadrant. A bright band is visible in the radar reflectivity data at around 1 km height,
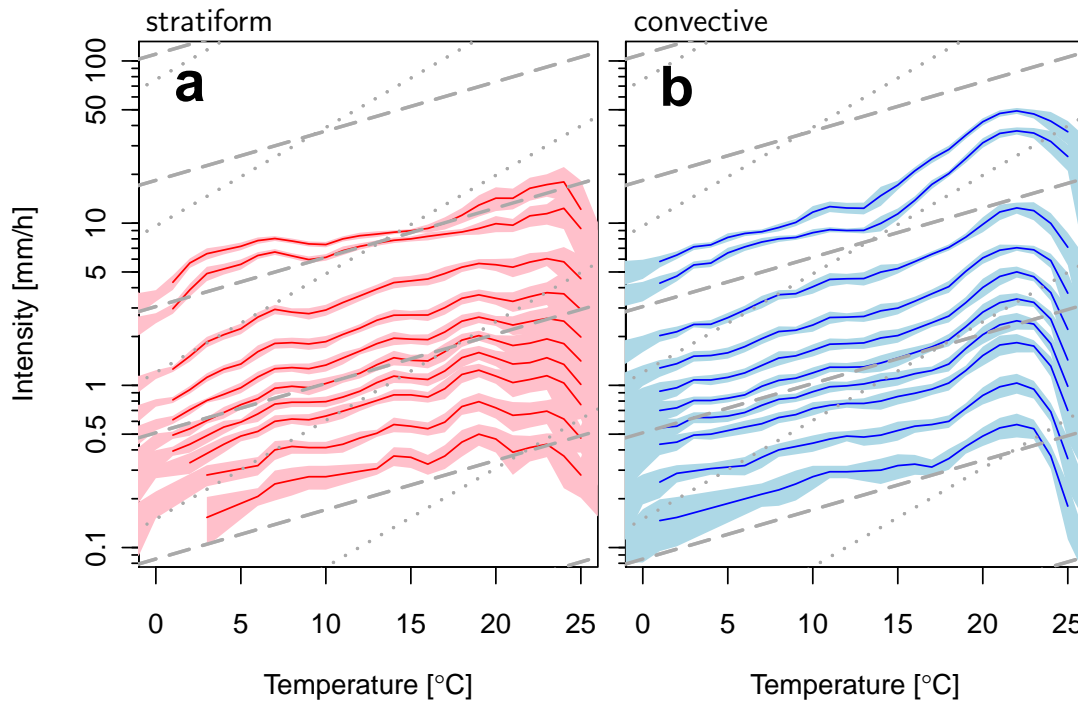
8

Figure S4: **Temperature dependence for radar data.** Precipitation intensities for the $\{50^{th}, 60^{th}, 70^{th}, 75^{th}, 80^{th}, 85^{th}, 90^{th}, 95^{th}, 99^{th}, 99.5^{th}\}$ percentiles, from bottom to top in panels. **a**, stratiform precipitation. **b**, convective precipitation. Dashed (dotted) gray lines mark 7%/°C (14%/°C) increases. Curves derived from the radar data with $2\ K$ temperature bins and intensity cutoff $0.1\ mm/h$. This lower cutoff – compared to the station data – explains the relative vertical shift of the curves compared to those in Fig. 2c (main article). Note the logarithmic vertical axis.

9

most pronounced in the afternoon and evening hours. The Doppler velocity profile (Fig. S5b) shows the onset of rain as dark black regions (negative vertical velocity). Superimposed in Fig. S5b (red area) we show the melting layer. In Fig. S5c we show also the rain rate measured at the radar station, and the symbols for synoptic classification along with our overall classification for the North-Eastern quadrant. The classification confirms that stratiform conditions prevail in the regime exhibiting the bright band, hence our classification is consistent with this detection method.

We also contrast with a case of convective conditions (Fig. S5d-f). This event corresponds to the radar image shown in Fig. 1c, main text, where widespread convective conditions are present in the North-Eastern quadrant. The radar reflectivity (Fig. S5d) now shows a dominant vertical structure in the mid-afternoon, no clear horizontal structure is visible in this figure. A melting layer is still detectable, but its structure is horizontally much less homogeneous than for stratiform conditions (Fig. S5b).

An analysis of the data from 2007-2008 showed that the classification using vertical radar data was overall best in conditions where one of the two types (stratiform or convective) was dominant in the entire quadrant, i.e. in cases of a spatially homogeneous signal. In other cases, mixed conditions (both in space and time) can occur and the classification using the radar data alone is more difficult. However, these conditions correspond to data which has generally been discarded from our analysis as we only consider spatially homogeneous cases (Methods section of main text). With rapidly improving remote-sensing technology, the vertical data and the bright band condition is a promising route towards automatically detecting weather types. A challenge is, however, the limited spatial coverage of such data, as the vertical resolution decreases with horizontal distance from the station. A bright band is on the order of a few hundred metres deep, and is thus only distinguishable near the radar station [6, 7].

Supplementary Discussion

Comparison of observed event average with randomised average

In the main text we state that correlations of precipitation within an event could cause greater extremes in the event statistics than when such correla-
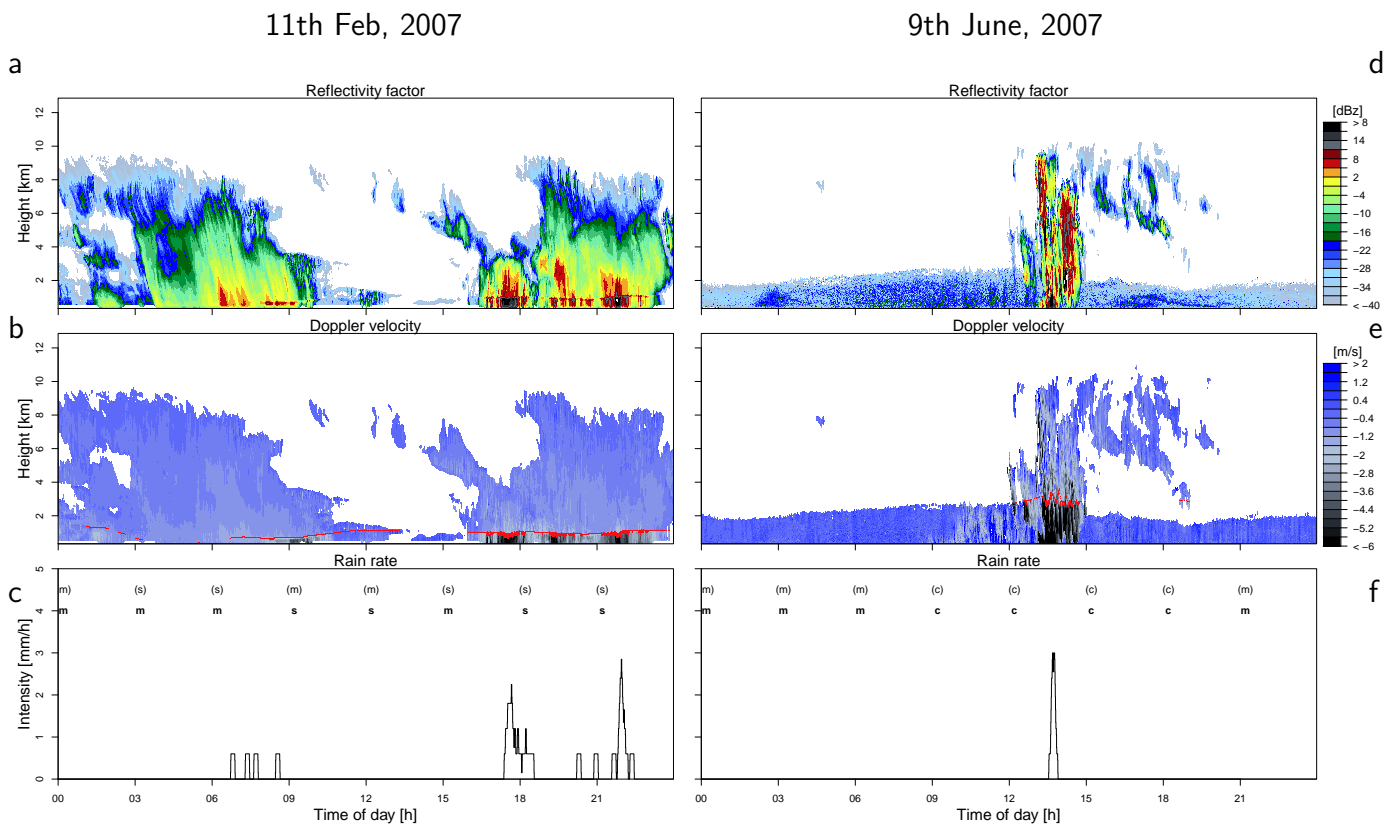
10

Figure S5: **Comparison with bright band method. a**, Radar reflectivity factor for a typical stratiform synoptic condition for one day (11th February, 2007) as measured at the Lindenberg station ($52°$ $9'$ N, $14°$ $10'$ O). **b**, as (a) but for Doppler velocity. **c**, Rain rate and classifications at the station location (bold) and overall classification in the North-Eastern quadrant (in parentheses); **d-f**, Same as a-c but for a typical convective event (9th June, 2007).

11

tions are absent. To check directly how large this effect is, we sample data from the rain gauge intensity distributions by randomly selecting 5-minute precipitation intensities. For example, for each pair of sampled values, we are able to compose a randomised event of 10 min duration and compute the average. We repeat this procedure a large number of times. To yield a fair comparison, we sample data only from a subset of data stemming from events with similar temperature and duration. In short, this corresponds to re-shuffling all data within a given event by replacing it with data from other events of the same duration and temperature. If the data within any given event were uncorrelated, this re-shuffling would leave the statistics of the event means unaltered.

The results for events of different durations – shown in Fig. S6b – indicate that the mean intensity of the resulting event will generally even out occasional extremes. This is especially the case for long durations, where the distribution becomes sharply peaked. At the cross-over of curves it is equally likely to observe short or long events of the given mean intensity. However, when event intensities are correlated, then events containing the extremes of Fig. 2a (main text) are more likely to contain other records of high intensity.

When comparing the original data in Fig. S6a with the randomly sampled data in Fig. S6b, we find that both convective and stratiform events are temporally correlated, i.e. the distribution of event means is wider than in the randomly sampled data. When comparing the average event intensity corresponding to events of increasing duration (light to dark curves in Fig. S6a, along arrows) stratiform rain (red) exhibits a cross-over of curves with different duration. This cross-over is reminiscent of sampling from the intensity distributions and means that the longer events produce more moderate average precipitation intensity than the smaller events. Conversely, convective precipitation (blue) shows no sign of such a cross-over up to the highest observed intensities.

Precipitation Yield

We have also computed the precipitation yield, which we define as the total amount of precipitation obtained for any of the two precipitation types at a given event-duration within one year. Precipitation yield is obtained as the product of the total count of observations per year at any given duration, the corresponding mean intensity (Fig. 4d) and the value of duration. The results are shown in Fig. S7a. This plot shows that convective precipitation produced
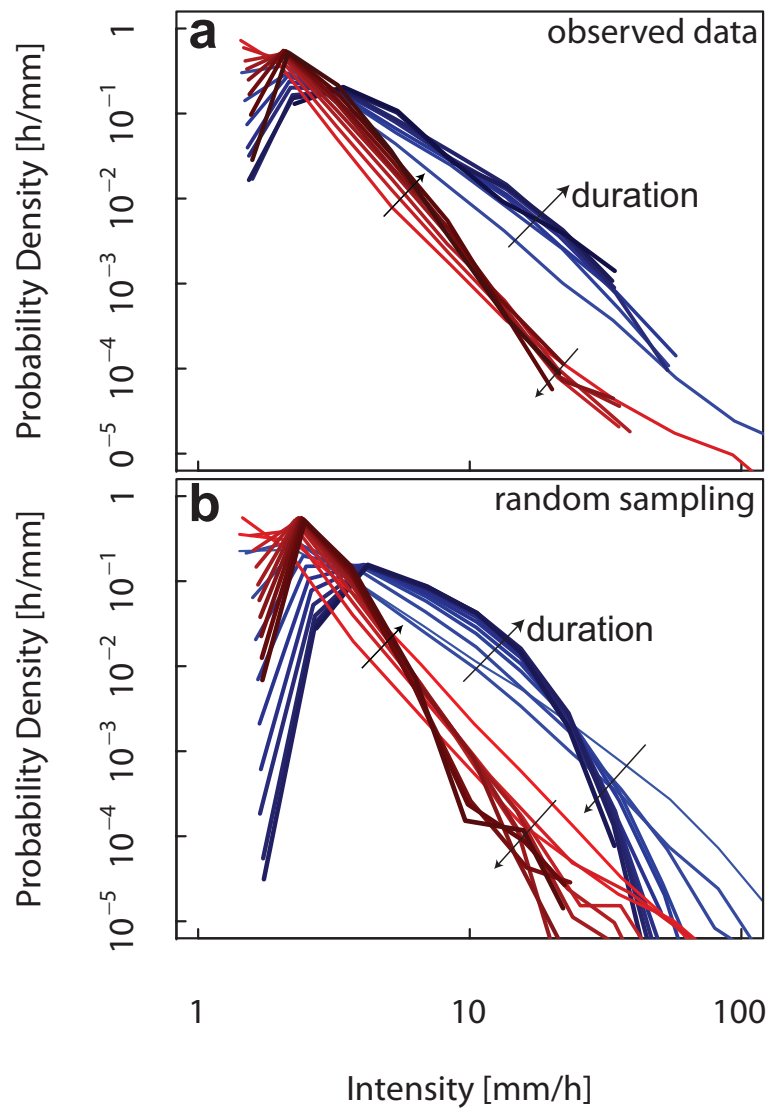
12

Figure S6: **Event correlations for station data. a**, Probability density functions of event intensity conditional on event duration for station data. Blue (red) shades correspond to convective (stratiform) precipitation. Durations range from 10–55 minutes for bright to dark colours (along arrows). **b**, Same as (a) but for randomised events where data from Fig. 2a were used to randomly compose events of durations corresponding to (a).
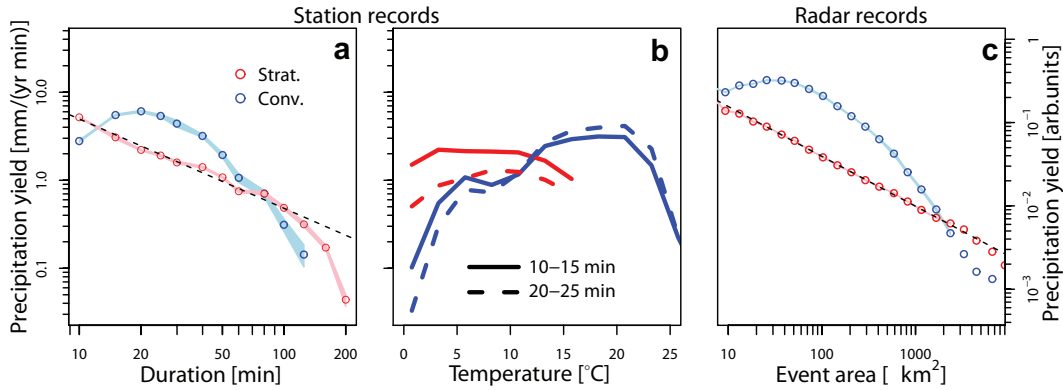
13

Figure S7: **Event scaling in space and time. a**, Convective (blue) and stratiform (red) precipitation yield as function of duration for station data. **b**, Temperature dependence of precipitation yield for station data conditional on two duration bins (10–15 and 20–25 minutes, see legend). **c**, similar to (a) but for radar measurements and event area. Dashed black lines indicate power-law fits to stratiform precipitation data.

the largest amount of precipitation through events of intermediate durations (near 25 minutes), hence again at a characteristic time scale. Analogous to Fig. 4 (main text) we also show the temperature (Fig. S7b). The temperature dependence is similar to that of the occurance of events (Fig. 4b, main text) but the curve of convection is substantially boosted by the weighting with intensity. Fig. S7c again shows the radar analog as function of event area and should be compared to the very similar Fig. S7a. Note that by the normalisation condition for probability density, the units of the curves in Fig. S7c become $mm/(yr\ min)$. In Fig. S7c arbitrary units are used due to the presence of missing values in the data.

14

Relative Humidity

To investigate the relationship between relative humidity, temperature and precipitation, we use data for eight additional rain gauge stations located in South Western Germany. The corresponding precipitation data are of half-hourly temporal resolution (which is the reason they were not included in the main analysis), and we have obtained matching hourly relative humidity for the time period 1997–2004. We then used the classification of stratiform and large scale synoptic conditions to separate the time series into these two types.

Fig. S8a and b presents scatter plots of relative humidity vs. temperature conditional on stratiform and convective precipitation, respectively. To obtain these plots, we have used only the dry intervals immediately before the onset of a precipitation event. Fig. S8a shows that stratiform precipitation occurs at times of overall high relative humidity and is approximately constant as a function of temperature. This result corresponds to approximately exponentially increasing values of specific humidity with temperature. Conversely, when conditioning on convective events (Fig. S8b), relative humidity decreases as a function of temperature. Overall, relative humidity is lower for this case than for stratiform conditions. It may hence be the process of vertical motion and the dynamics of moisture entrainment in convective updrafts that are likely to cause the exceedence of the Clausius-Clapeyron rate seen in Fig. 2c. Our results should be compared to recent studies of the dew-point temperature [10].

When considering only dry convective cloud conditions, (Fig. S8c), we find that relative humidity is markedly lower in comparison to conditions preceding convective precipitation (Fig. S8b). However, the overall behaviour for dry conditions still is characterised by a decline of relative humidity with temperature. We conclude that increases in convective precipitation intensity can not sufficiently be inferred from a simple analysis of near-surface relative humidity alone.
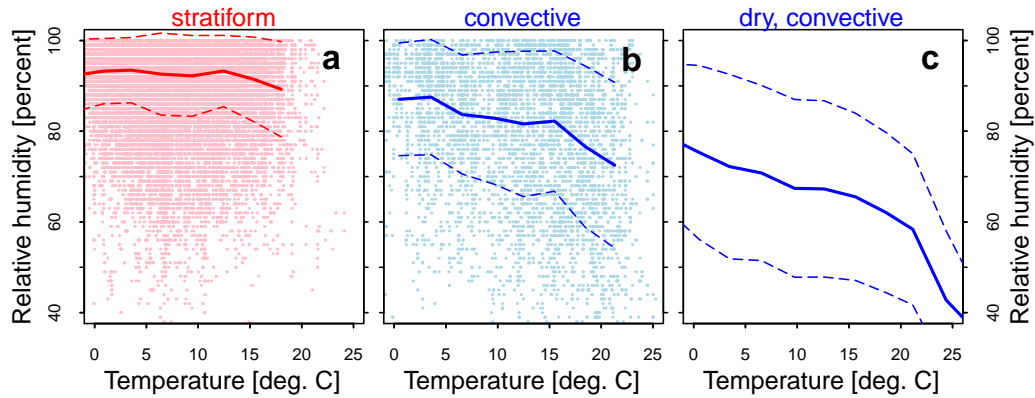
15

Figure S8: **Relative humidity as function of temperature. a**, Scatter plot of relative humidity vs. temperature for stratiform records, conditional on precipitation. Solid (dashed) lines indicate the mean (mean $\pm$ one standard deviation) of relative humidity for every four degrees Celsius temperature bin. **b**, Same as (a) but for convective precipitation. **c**, Same as (a) but for convective cloud conditions without precipitation. Note that we have removed the scattered data in (c) for clarity of presentation.

References

[1] Dai, A., Lin, X. & Hsu, K.-L. The frequency, intensity, and diurnal cycle of precipitation in surface and satellite observations over low- and mid-latitudes. *Clim. Dyn.* **29**, 727–744 (2007).

[2] Dai, A., Giorgi, F. & Trenberth, K. E. Observed and model-simulated diurnal cycles of precipitation over the contiguous united states. *J. Geophys. Res.* **104**, 6,377–6,402 (1999).

[3] Lenderink, G. & van Meijgaard, E. Increase in hourly precipitation extremes beyond expectations from temperature changes. *Nature Geosci.*

16

1, 511–514 (2008).

[4] Berg, P. *et al.* Seasonal characteristics of the relationship between daily precipitation intensity and surface temperature. *J. Geophys. Res.* **114**, D18102 (2009).

[5] Haerter, J. O. & Berg, P. Unexpected rise in extreme precipitation caused by a shift in rain type? *Nature Geosci.* **2**, 372–373 (2009).

[6] Steiner, M., Houze Jr., R. A. & Yuter, S. E. Climatological characterization of three-dimensional storm structure from operational radar and rain gauge data. *J. Appl. Met.* **34**, 1,978–2,007 (1995).

[7] Houze Jr, R. Stratiform precipitation in regions of convection: A meteorological paradox? *B. Am. Meteorol. Soc.* **78**, 2,179–2,226 (1997).

[8] Smyth, T. & Illingworth, A. Radar estimates of rainfall rates at the ground in bright band and non-bright band events. *Q. J. Roy. Meteor. Soc.* **124**, 2,417–2,434 (1998).

[9] Illingworth, A. *et al.* Continuous evaluation of cloud profiles in seven operational models using ground-based observations. *B. Am. Meteorol. Soc.* **88**, 883–898 (2007).

[10] Lenderink, G., Mok, H. Y., Lee, T. C. & van Oldenborgh, G. J. Scaling and trends of hourly precipitation extremes in two different climate zones – Hong Kong and the Netherlands. *Hydrol. Earth Syst. Sci.* **15**, 3,033–3,041 (2011).

17